


# Amino-terminal enhancer of split gene *AES* encodes a tumor and metastasis suppressor of prostate cancer

Yoshiyuki Okada,<sup>1,2,4</sup> Masahiro Sonoshita,<sup>1,4</sup> Fumihiko Kakizaki,<sup>1,4</sup> Naoki Aoyama,<sup>1,4</sup> Yoshiro Itatani,<sup>1,4</sup> Masayuki Uegaki,<sup>2</sup> Hiromasa Sakamoto,<sup>2</sup> Takashi Kobayashi,<sup>2</sup> Takahiro Inoue,<sup>2</sup> Tomomi Kamba,<sup>2</sup> Akira Suzuki,<sup>3</sup> Osamu Ogawa<sup>2</sup> and M. Mark Taketo<sup>1,4</sup> 

Departments of <sup>1</sup>Pharmacology; <sup>2</sup>Urology, Kyoto University Graduate School of Medicine, Kyoto; <sup>3</sup>Division of Cancer Genetics, Medical Institute of Bioregulation, Kyushu University, Fukuoka, Japan

## Key words

Androgen receptors, neoplasm invasiveness, neoplasm metastasis, prostatic neoplasms, transcription factors

## Correspondence

Makoto Mark Taketo, Division of Experimental Therapeutics, Kyoto University Graduate School of Medicine, Yoshida-Konoé-cho, Sakyo-ku, Kyoto 606-8501, Japan. Tel: +81-75-753-4391; Fax: +81-75-753-4402; E-mail: taketo@mfour.med.kyoto-u.ac.jp

<sup>4</sup>Present Address: Division of Experimental Therapeutics, Kyoto University Graduate School of Medicine, Yoshida-Konoé-cho, Sakyo-ku, Kyoto, 606-8501, Japan

## Funding Information

Japan Society for the Promotion of Science, Grant / Award Number: 'Kiban A/25253022'.

Received December 20, 2016; Revised February 1, 2017; Accepted February 2, 2017

*Cancer Sci* 108 (2017) 744–752

doi: 10.1111/cas.13187

A major cause of cancer death is its metastasis to the vital organs. Few effective therapies are available for metastatic castration-resistant prostate cancer (PCa), and progressive metastatic lesions such as lymph nodes and bones cause mortality. We recently identified *AES* as a metastasis suppressor for colon cancer. Here, we have studied the roles of *AES* in PCa progression. We analyzed the relationship between *AES* expression and PCa stages of progression by immunohistochemistry of human needle biopsy samples. We then performed overexpression and knockdown of *AES* in human PCa cell lines LNCaP, DU145 and PC3, and determined the effects on proliferation, invasion and metastasis in culture and in a xenograft model. We also compared the PCa phenotypes of *Aes/Pten* compound knockout mice with those of *Pten* simple knockout mice. Expression levels of *AES* were inversely correlated with clinical stages of human PCa. Exogenous expression of *AES* suppressed the growth of LNCaP cells, whereas the *AES* knockdown promoted it. We also found that *AES* suppressed transcriptional activities of androgen receptor and Notch signaling. Notably, *AES* overexpression in AR-defective DU145 and PC3 cells reduced invasion and metastasis to lymph nodes and bones without affecting proliferation in culture. Consistently, prostate epithelium-specific inactivation of *Aes* in *Pten<sup>flox/flox</sup>* mice increased expression of *Snail* and *MMP9*, and accelerated growth, invasion and lymph node metastasis of the mouse prostate tumor. These results suggest that *AES* plays an important role in controlling tumor growth and metastasis of PCa by regulating both AR and Notch signaling pathways.

In many types of cancer, the major cause of cancer death is metastasis to the vital organs. Prostate cancer (PCa) is the most common male malignancy and the second leading cause of cancer death of men in the Western world.<sup>(1,2)</sup> Currently, advanced PCa is treated by androgen ablation therapy. While it is usually effective in the beginning, most PCa patients develop resistance to the therapy sooner or later.<sup>(3)</sup> Once the disease reaches the castration-resistant stage, there are few effective therapies, and the uncontrolled metastatic lesions cause mortality, including those to regional lymph nodes and distant organs such as bones. Unlike other epithelial tumors that metastasize to the bone only occasionally, metastatic PCa almost invariably targets the bone, and displays characteristic osteoplastic rather than osteolytic lesions.<sup>(4)</sup>

In both normal prostate physiology and PCa, androgen receptor (AR) mediates key signaling as a nuclear hormone receptor.<sup>(5)</sup> AR is expressed in most PCa cases, and dysregulation of its downstream growth control mechanism plays a significant role in tumorigenesis and metastasis of PCa.<sup>(6,7)</sup>

In the normal growth and development of the prostate, Notch signaling plays a critical role.<sup>(8)</sup> Several lines of evidence

indicate that abnormal expression of Notch receptor and/or ligands is often associated with the progression and metastasis of PCa<sup>(9–12)</sup> including frequent metastasis to the bone.<sup>(13)</sup>

Amino-terminal enhancer of split (*AES*), also called *Grg5* in mice, is a distinct member of the Groucho/Transducin-Like Enhancer of split (*Gro/TLE*) gene family, with its Q/GP domains showing similarities to those in *TLEs*.<sup>(14,15)</sup> We demonstrated earlier that *AES* suppresses colon cancer metastasis through Notch signaling inhibition.<sup>(16)</sup> It was also reported that *AES* regulates AR transcriptional activity. For example, it disrupts the interaction between AR N- and C-terminal domains, inhibiting AR–DNA interaction.<sup>(17,18)</sup> But the role of *AES* in PCa has not been investigated fully.

Alterations in the *PTEN/PI3K/AKT* pathway are implicated in PCa development, with approximately 70% of late-stage tumors showing loss of *PTEN* or activation of phosphoinositide 3-kinase (*PI3K*).<sup>(19)</sup> *Pten*-deficient mice develop PCa through prostatic intraepithelial neoplasia (*PIN*), and are thought to mimic human PCa.<sup>(20)</sup> In the present study, we have investigated the roles of *AES* in PCa in both humans and mice.

**Table 1. Inverse correlation between AES expression levels and metastatic spread extents in human PCa. AES expression in the primary tumors of 82 patients was evaluated by immunohistochemistry as positive (+) or negative (–)**

Clinicopathological factors	AES expression		P-value
	+(n = 55)	–(n = 27)	
Age (years)	71.5 ± 1.2	73.0 ± 1.5	0.95*
PSA (ng/mL)	424 ± 244	310 ± 80	0.66*
Lymph node involvement			
Positive	12	12	0.042†
Negative	43	15	
Bone metastasis			
Positive	18	14	0.097†
Negative	37	13	
Stage			
Localized	32	9	0.03†
Metastatic	23	18	

\*Mann–Whitney U-test, †Fisher's exact test.

## Materials and Methods

**Characteristics of PCa patients.** Formalin-fixed, paraffin-embedded (FFPE) sections of primary tumors were obtained from 82 men who underwent prostate needle biopsy with informed consents signed as approved by the Kyoto University Ethics Committee (G52), and consequently were diagnosed to have PCa at Kyoto University Hospital. Patient characteristics are shown in Table 1. Decalcified FFPE sections of bone metastasis lesions were obtained from nine PCa patients who underwent a palliative surgery (mostly decompression laminectomy) for vertebral bone metastasis. All nine patients were on androgen deprivation therapy (ADT) and had developed castration-resistant disease at the time of surgery.

**Mouse strains.** Mice with the following genotypes were used: a conditional allele for *Pten* (*Pten<sup>fl/fl</sup>* in C57Bl/6 background) with loxP sites flanking exon 5,<sup>(21)</sup> a conditional allele for *Aes* with loxP sites flanking Exon2 of *Aes*,<sup>(16)</sup> a *Probasin-Cre* allele (*TgPbsn<sup>Cre</sup>* in C57Bl/6 background) having Cre recombinase gene placed under the control of *Probasin* promoter,<sup>(22)</sup> obtained from NCI.

**Histological, immunohistochemical and immunofluorescent analyses.** Tissues were fixed in 4% paraformaldehyde, embedded and sectioned at a thickness of 4 μm for histological, immunohistochemical (IHC), and immunofluorescent analyses. These sections were stained with hematoxylin and eosin (H&E) or processed further for immunostaining as described previously.<sup>(23)</sup> For immunofluorescence staining, Alexa Fluor 594-conjugated goat anti-mouse IgG or 488-conjugated goat anti-rabbit IgG (Molecular Probes, Invitrogen, Carlsbad, CA) was used as the secondary antibody. Bright-field and fluorescence images were captured with Olympus DP73 (Olympus, Tokyo, Japan) or Leica CTR6000 fluorescent microscope (Leica, Wetzlar, Germany) and analyzed using Adobe Photoshop software (Adobe, San Jose, CA, USA).

Microinvasion of the mouse prostate tumor cells were defined as broken basement membrane by tumor cells infiltrated into the interstitial space. Microinvasion was counted in three randomly selected light microscopy fields at 100× magnification for each section. Cells positive for nuclear Ki67 immunostaining were counted, and the proportion of Ki67-positive cells in at least 200 cells was determined for the

positive cell frequency. The extent of AES immunohistochemical staining was validated using the intestinal polyp tissue from *Apc<sup>4716</sup>* polyposis mice<sup>(16)</sup> as positive control, whereas the prostate tumor tissue from *TgPbsn<sup>Cre</sup>;Pten<sup>fl/fl</sup>;Aes<sup>fl/fl</sup>* mice as negative control. It was scored as none (negative control), weak (positive but weaker than positive control), moderate (as strong as positive control) or strong (stronger than positive control) as shown in the representative images (Fig. S1).

**Cell culture, and proliferation and invasion assays.** PCa cell lines LNCaP, PC3, and DU145 were purchased from American Type Culture Collection (ATCC, Manassas, VA, USA) and cultured in RPMI 1640 with 10% fetal bovine serum (FBS). Cell proliferation in culture was evaluated using Cell Counting Kit-8 (Dojindo, Kumamoto, Japan).

For Matrigel invasion assays, cells were serum starved for 6 h and suspended in serum-free RPMI 1680. The cell suspension ( $5 \times 10^4$  cells) was then added to the Matrigel-coated 8.0-μm pore polyethylene terephthalate filter insert of a 24-well cell culture chamber (BD Falcon, Franklin Lakes, NJ, USA) and was incubated for 24 h with the medium containing 10% FBS in the bottom chamber. Residual cells on the upper side of chambers were removed by scraping with cotton swabs and the cells that attached to the lower side of the membrane were fixed with 70% ethanol and stained with H&E. Invaded cells were counted under light microscopy.

**Animal experiments.** All experiments using animals were performed according to the protocols approved by Animal Research Committee of Kyoto University. Mice were housed in a specific pathogen-free room.

To assess the influence of *Aes* on prostate tumor development, male *TgPbsn<sup>Cre</sup> Pten<sup>+/+</sup> Aes<sup>+/+</sup>* (wild-type), *TgPbsn<sup>Cre</sup> Pten<sup>fl/fl</sup> Aes<sup>+/+</sup>* (*Pten*), *TgPbsn<sup>Cre</sup> Pten<sup>fl/fl</sup> Aes<sup>fl/fl</sup>* (*Aes/Pten*) mice ( $n = 5$  for each) were sacrificed at 3, 6, 12, and 18 months of age and the genitourinary complex (bladder, urethra, prostate glands, and seminal vesicles) was excised and photographed. Then, each prostatic lobe was dissected, weighed, and subjected to further experiments. Samples were snap-frozen in liquid nitrogen for western blot analyses and isolation of RNA or genomic DNA. At dissection, the intraperitoneal cavity was also carefully inspected for any metastatic lesions. The lungs and liver were excised and subjected to histopathological examinations.

For *in vivo* transplantation models, we generated PCa cells that stably expressed firefly luciferase, and *Aes* or none (control). Cells were collected by trypsinization and centrifugation at 1000 g, resuspended in PBS and kept on ice until injection. In the cardiac injection model, 6-week-old male nude mice (Clea, Japan) were anesthetized and  $5 \times 10^5$  cells/mouse were injected into the left ventricle as described previously.<sup>(24)</sup> Correct injection into the systemic circulation was confirmed by the lack of photon flux from the injection site detected by an *in vivo* imaging system (IVIS, Xenogen, Alameda, CA, USA) 2 min after each injection. In the orthotopic inoculation model, 6-week-old male NOD/SCID mice (Clea, Japan) were anesthetized and  $1 \times 10^6$  cells were injected into the anterior prostate as described previously.<sup>(25)</sup>

In the femur implantation model, 6-week-old male nude mice (Clea, Japan) were anesthetized and  $1 \times 10^6$  cells were injected into the left femur body as described previously.<sup>(26)</sup> Following injections, mice were monitored daily for their general condition, and the extent of bone metastasis was determined on post-injection days 14, 28, and 42 by injecting luciferin intraperitoneally followed by photon flux determination using IVIS. The mice were euthanized, and bones,

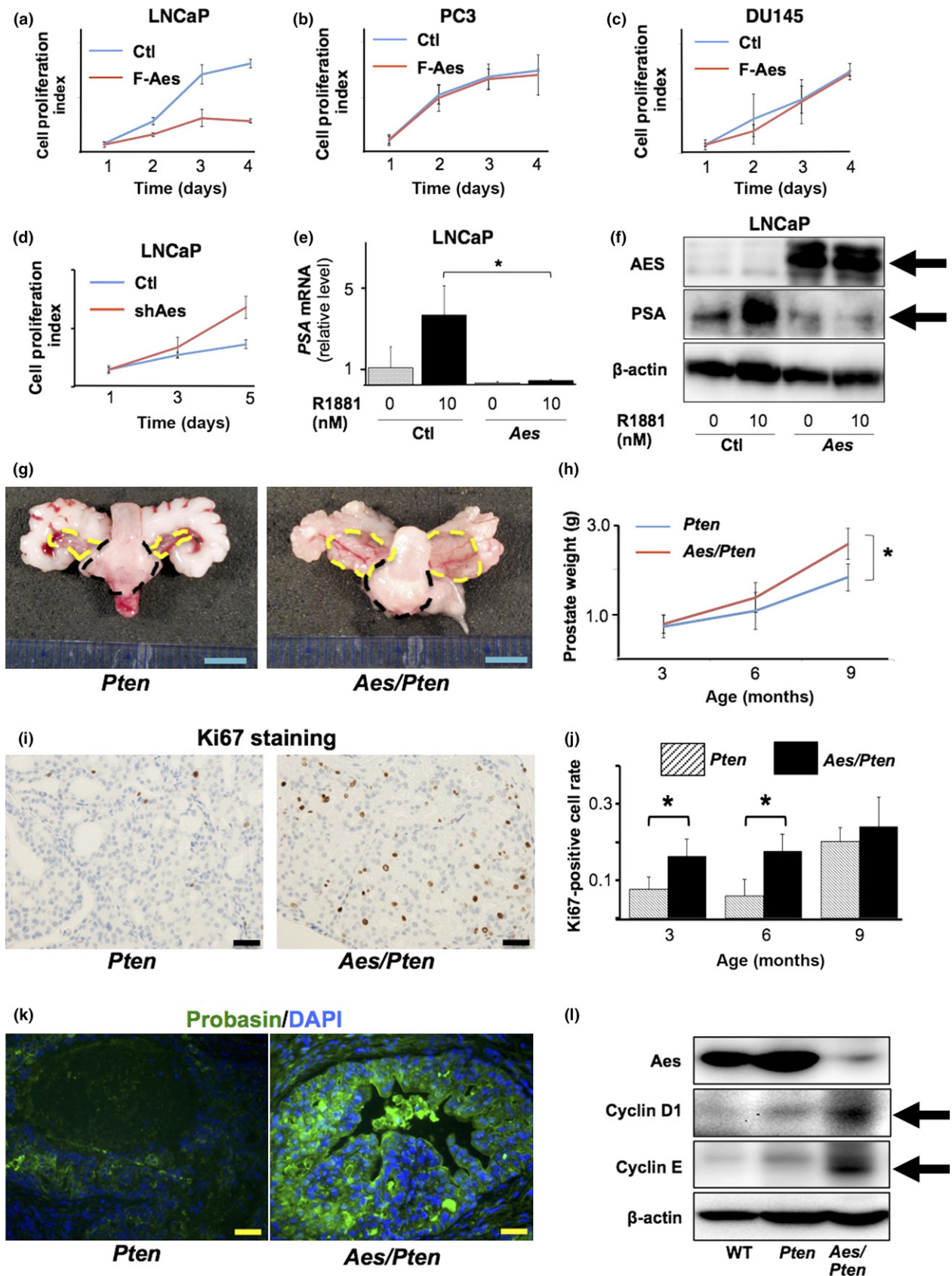


**Fig. 1.** *Aes* suppresses growth of PCa through androgen receptor inhibition. (a–c) Effects of *Aes* overexpression on the growth of PCa cell lines determined by MTT assay; (a) LNCaP, (b) PC3, (c) DU145. F-*Aes*, flag-tagged *Aes*; Ctl, no-*Aes* control vector. Note that LNCaP expresses AR whereas either PC3 or DU145 does not. (d) Effects of *Aes* knockdown by shRNA against *AES* mRNA (sh*Aes*) on the growth of LNCaP determined by MTT assay. (e) Expression levels of PSA mRNA in LNCaP determined by q-RT-PCR, in the absence (0 nM) or presence (10 nM) of synthetic androgen R1881 with exogenous expression of *Aes* (*Aes*) or none (Ctl). (f) Western analysis of PSA protein in LNCaP cells upon expression of exogenous *Aes*. Arrows indicate the positions of the authentic proteins. (g) Dissection micrographs of prostates from *Pten*<sup>fl/fl</sup> *PbCre* mice (*Pten*) and *Aes*<sup>fl/fl</sup> *Pten*<sup>fl/fl</sup> *PbCre* mice (*Aes/Pten*) at 6 months of age. Yellow circles indicate anterior prostate, whereas black ones show ventral and lateral prostate. Ruler is in mm. (h) Prostate weights of *Pten* and *Aes/Pten* mice at 3, 6 and 9 months of age. ( $n = 5$ , for each age group) (i) Immunohistochemical staining for Ki67 in *Pten* and *Aes/Pten* mouse prostates at 6 months of age. Scale bar 20  $\mu$ m. (j) Quantification Ki67-positive cells for PIN in *Pten* and *Aes/Pten* mice at 3, 6 and 9 months of age. (k) Immunofluorescence staining for probasin (green) and nuclear DAPI (blue) in *Pten* and *Aes/Pten* mouse prostates. Scale bar 20  $\mu$ m. (l) Western analysis of cyclin D1 and cyclin E in wild-type (WT) and mutant mouse prostates.  $\beta$ -actin was used as the loading control. Arrows indicate the positions of the authentic proteins. Asterisks (\*) show the statistical significance ( $P < 0.05$ ).

prostates and other organs with tumor involvement detected by IVIS were collected, fixed in formalin, and embedded in paraffin. Metastatic tumors were identified in sections under a light microscope.

**Western blotting.** For Western blots, tissues or cells were lysed in the NP-40 lysis buffer containing 20 mM Tris-HCl (pH 7.5), 150 mM NaCl, 10% glycerol, 1% Nonidet P-40, 10 mM sodium fluoride, 1 mM sodium pyrophosphate, 1 mM sodium orthovanadate, and Complete protease inhibitor (Roche Applied Science). Lysates containing 20 or 40  $\mu$ g of protein were separated by SDS/PAGE and transferred to Immobilon P membranes (Millipore, Billerica, MA, USA). Membranes were blocked with 5% nonfat dry milk (in Tris-buffered saline, 0.05% Tween-20) for 1 h at room temperature. They were then probed with the primary antibodies for at 4°C 8 h. After incubation with horseradish peroxidase-conjugated secondary antibodies (anti-mouse IgG, Pierce, Rockford, IL; anti-rabbit IgG, GE Healthcare Amersham, Buckinghamshire, UK), bound proteins were detected by incubation with Immobilon chemiluminescent substrate (Millipore).

**Antibodies.** Anti-*Aes* antibody was described previously.<sup>(16)</sup> Goat polyclonal anti-prostate-specific antigen (PSA) was purchased from Santa Cruz Biochemistry (Santa Cruz, CA, USA), mouse polyclonal  $\beta$ -actin from SIGMA (A5316), mouse polyclonal Cyclin D1 from BD (556470), mouse monoclonal anti-Cyclin E1 from Santa Cruz (sc-248), goat polyclonal anti-Probasin from Santa Cruz (sc-17126), rat monoclonal anti-Hes1 from MBL (D134-3), rabbit monoclonal anti-Snail from CST (C15D3), rabbit polyclonal anti-EZH2 from CST (4905S), and rabbit polyclonal anti-MMP9 from Abcam (ab38898).

**Quantitative RT-PCR (q-RT-PCR).** q-RT-PCR was performed using an ABI StepOnePlus (Applied Biosystems, Foster City, CA, USA). We used the following primer sets and probes: human *AES* primers (F, forward, 5'-TCCCTTTTCTTTGACAGATGGG-3'; and R, reverse, 5'-AGGAGTCCGAGGTGGTG AATT-3') and probe (5'-CTCCTCGCACCTACCCAGCA ACTC-3'), mouse *Aes* primers (F, 5'-GGCGGAAATTGTG AAGAGGCT-3'; R, 5'-CTTGGCTCTCTCGATGGCTC-3') and probe (5'-TTTGC GCCAGGTTCTGCCC-3').

Levels of human *ribosomal S18 RNA*, human *ACTB*, and mouse *Gapdh* were determined using Taqman Ribosomal RNA, human  $\beta$ -actin and rodent GAPDH Control Reagents (Applied Biosystems). Reactions were prepared using Taqman Universal PCR Master Mix (Applied Biosystems). Relative transcript levels were calculated by the comparative  $C_T$  method (ABI User Bulletin #2). Primers used were as follows, *HES1* (111 bp); F, 5'-TCAACACGACACCGGATAAA-3' and R, 5'-TCAGCTGGCTCAGACTTTCA-3', *PSA* (74 bp); F, 5'-GGAAATGACCAGGCCAAGAC-3' and R, 5'-CAA CCCTGGACCTCACACCTA-3'.

**Reporter activity assays.** Notch1 transcription activity was evaluated using Notch reporter assay. Cultured cells were transfected with pGa981-6 luciferase reporter<sup>(27)</sup> simultaneously with *Aes* or control (Mock) expression vector with or without RAMIC.<sup>(16)</sup> Twenty-four hours after transfection, luciferase activities were determined using Dual-Luciferase Reporter Assay System (Promega) according to the manufacturer's protocol with a MITHORAS LB 940 luminometer (Berthold Biolumat, Bad Wildbad, Germany). Firefly luciferase activities were normalized against those of *Renilla* luciferase.

**Statistical analyses.** Each experimental series was performed at least in triplicate, and the results are presented as means  $\pm$  SEM. Student's *t*-test, Fisher's exact test and a logistic regression test were employed using commercially available software (SPSSII, SPSS, Tokyo, Japan Inc.). All tests were two-sided and *P*-values  $< 0.05$  were considered statistically significant.

## Results

**AES levels in primary PCa are inversely correlated with extents of progression and metastasis.** We have recently found that *AES* suppresses colon cancer metastasis through inhibition of Notch signaling.<sup>(16)</sup> PCa data extracted from a gene expression database show that *AES* expression is down-regulated in PCa in a stage-dependent manner (Fig. S2),<sup>(19)</sup> suggesting that *AES* is a candidate tumor and/or metastasis suppressor in PCa.

To test the possibility, we examined human PCa tissues for *AES* expression by IHC, and asked whether its expression is associated with clinical aggressiveness of PCa. We analyzed needle biopsy specimens of the prostate obtained from 82 untreated PCa patients, and found that *AES* expression levels were inversely correlated with lymph node involvement and clinical stage of PCa (Table 1). In this patient population, *AES*-negative PCa had twice higher frequency of lymph node involvement, which was statistically significant (44% vs 22%,  $P = 0.042$ ). Additionally, *AES*-negative PCa was more likely to have bone metastasis than *AES*-expressing PCa, although the difference was not statistically significant (52% vs 33%,  $P = 0.097$ ). Overall, 67% of patients with PCa lacking *AES* expression had metastasis, whereas only 42% of those expressing *AES* did ( $P = 0.03$ ). On the other hand, *AES* expression was not significantly associated with the PSA level or Gleason grade (data not shown) suggesting that *AES* expression is an independent biomarker that predicts metastatic spread of PCa. Indeed, after adjusting to the Gleason score, expression of *AES* was still significantly associated with lymph node involvement (odds ratio (OR) 2.79, 95% confidence interval (CI) 1.079–7.191,  $P = 0.0343$ , logistic regression test) as well as to metastasis (OR 2.87, 95% CI: 1.037–7.918,  $P = 0.0423$ ), except bone metastasis (OR 2.26, 95% CI: 0.894–5.723,  $P = 0.0848$ ).

Furthermore, AES expression was abrogated in 78% ( $n = 7$ ) of nine bone metastatic lesions (Fig. S3), whereas it was negative only in 44% ( $n = 14$ ) of primary prostatic lesions of PCA with bone metastasis.

**AES suppresses prostate tumor growth in culture and *in vivo* through androgen receptor inhibition.** To investigate the effects of AES expression on androgen activity, we first studied the relationship between tumor growth and AES expression using human PCA cells in culture. Exogenous expression of *Aes* inhibited the proliferation by approximately 50% in androgen-dependent LNCaP cells (Fig. 1a), whereas it did not affect the proliferation of AR-independent PC3 (Fig. 1b) or DU145 (Fig. 1c) cells. Consistently, silencing of *AES* by shRNA promoted the proliferation rate twice in LNCaP cells (Fig. 1d). These data suggest that AES reduces the proliferation of PCA cells through inhibition of AR activity.

Because it was reported that AES could inhibit the AR transcriptional activity,<sup>(17,18)</sup> we next tested whether AES blocked the AR activity by determining the expression levels of an AR target gene PSA upon androgen stimulation. As anticipated, q-RT-PCR (Fig. 1e) and Western blotting (Fig. 1f) demonstrated significant reductions in both mRNA and protein levels of PSA upon AES expression.

To investigate the inhibitory function of AES on prostate tumor growth *in vivo*, we crossed mice carrying a floxed allele of *Aes*<sup>(16)</sup> (*Aes*<sup>fl/fl</sup>) with PIN model mice with prostate-specific deletion of a tumor suppressor *Pten* under the control of *probasin* promoter (*TgPbsn*<sup>Cre</sup> *Pten*<sup>fl/fl</sup>). The latter model develops PIN in an androgen-dependent manner.<sup>(20,28)</sup> The weight of the prostate gland was 1.5–2 times heavier in *Aes/Pten* compound knock-out mice than that in *Pten* single knock-out mice (Fig. 1g,h) ( $P < 0.05$ ).

The enlarged prostate size in *Aes/Pten* mice was attributable to an increased growth of prostate epithelium as shown by larger area of PIN lesion in histology, and as evident by approximately twice higher density of Ki67-expressing cells in the prostatic epithelium of *Aes/Pten* mice compared with that of *Pten* littermates (Fig. 1i,j), suggesting accelerated proliferation of prostatic epithelial cells in *Aes/Pten* mice.

It has been reported that AR transcriptional activity is reduced by *Pten* loss-of-function mutation in the prostatic epithelial cells.<sup>(29)</sup> Consistently, we found that probasin was scarcely expressed in the prostatic epithelium of *Pten* mice by immunofluorescence analysis (Fig. 1k, left). Notably, expression of probasin was remarkably restored in that of *Aes/Pten* mice (Fig. 1k, right), suggesting that *Aes* suppressed AR

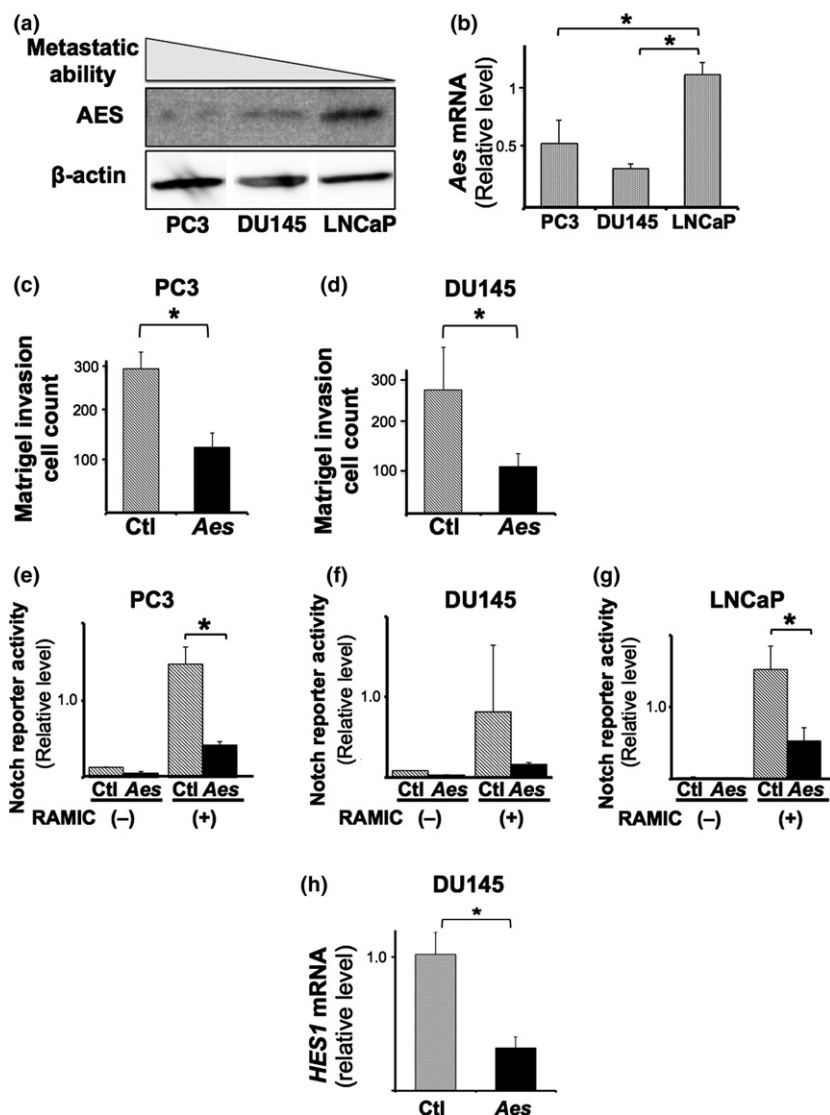


**Fig. 2.** AES suppresses PCA cell invasion through Notch signaling inhibition. (a) Expression of AES protein in PCA cell lines, PC3, DU145 and LNCaP, analyzed by western blotting. (b) Expression levels of AES mRNA in PC3, DU145 and LNCaP determined by q-RT-PCR. (c, d) Effects of *Aes* overexpression on Matrigel invasion in PC3 (c) and DU145 (d) PCA cell lines (per x200 field). (e–f) Effects of *Aes* overexpression on Notch reporter activity in PC3 (e), DU145 (f) and LNCaP (g) cell lines, either in the absence (–) or presence (RAMIC) of the recombinant form of activated Notch receptor. Ctl: no-*Aes* control vector. (h) Expression levels of *HES1* mRNA in DU145 determined by q-RT-PCR upon exogenous expression of *Aes* (*Aes*) or none (Ctl). In (b–h), asterisks (\*) show the statistical significance ( $P < 0.05$ ).

transcriptional activity in the *Pten*-deficient prostatic epithelium. It is known that activation of the AR promotes cell-cycle progression in the prostate epithelium and cancer cells.<sup>(7)</sup> Consistent with the AR activation by *Aes* loss-of-function mutation, cyclin family proteins were expressed more abundantly in the prostate of *Aes/Pten* mice than that of *Pten* mice (Fig. 11). Taken together, these results suggest that AES inhibits the proliferation of prostate tumor cells through AR inhibition.

**AES blocks PCa cell invasion through Notch signaling inhibition.** We previously reported that AES inhibits Notch signaling, and subsequently suppresses the invasion and metastasis of mouse colorectal cancer cells.<sup>(16)</sup> Western blotting revealed that the AES expression levels were inversely correlated with the metastatic ability<sup>(30)</sup> among three PCa cell lines (Fig. 2a, b). We also confirmed that all of PC3, DU145, and LNCaP cell lines express Notch1 and Notch2 receptors, and their ligands Jagged1 (data not shown) as reported previously.<sup>(31)</sup> We then assessed the effects of *Aes* overexpression on Matrigel invasion activity. Exogenous expression of *Aes* decreased the number of invading cells by 50%–70% in both PC3 (Fig. 2c) and DU145 (Fig. 2d) cell lines without affecting proliferation. In LNCaP cells, reduced invasion may be partly attributable to the inhibition of proliferation, which was reduced by ~50% upon exogenous expression of *Aes* (Fig. 1a).

We next determined the effects of *Aes* expression on Notch signaling transcription using a luciferase-reporter assay. Forced

expression of *Aes* suppressed the Notch reporter activity by 70%–90% in all three PCa cell lines either in the absence or presence of RAMIC, a recombinant form of activated Notch receptor (Fig. 2e–g). Moreover, exogenous expression of *Aes* caused approximately 70% reduction in the mRNA levels for *HES1*, one of the representative transcriptional targets of Notch signaling (Fig. 2h). Collectively, these results suggest that AES reduces Notch signaling transcription and cellular invasion also in PCa cells as in CRC cells.

**AES suppresses metastatic spread of human PCa cell grafts in mice.** To further investigate the role of AES in PCa metastasis *in vivo*, we next evaluated the effect of AES expression using two transplantation-metastasis mouse models. When injected into the cardiac left ventricle, PC3 and MDA-PCa2b cells can metastasize to bones such as the mandible, humerus and femur of nude mice. Notably, expression of *Aes* in PC3 cells significantly reduced (by ~50 times) the metastatic spread to the bone after cardiac injection when assessed with an *in vivo* photon-count imaging system (Fig. 3a–c).

Next we injected PC3 cells with or without exogenous *Aes* expression directly into the mouse femur to interrogate tumor growth between *Aes*-expressing and -nonexpressing PC3 cells in the bone. Notably, we found no significant difference between PC3 cells with and without exogenous *Aes* expression by this experimental design (Fig. 3d,e), suggesting that the less metastatic spread with *Aes*-expressing cells is attributable to

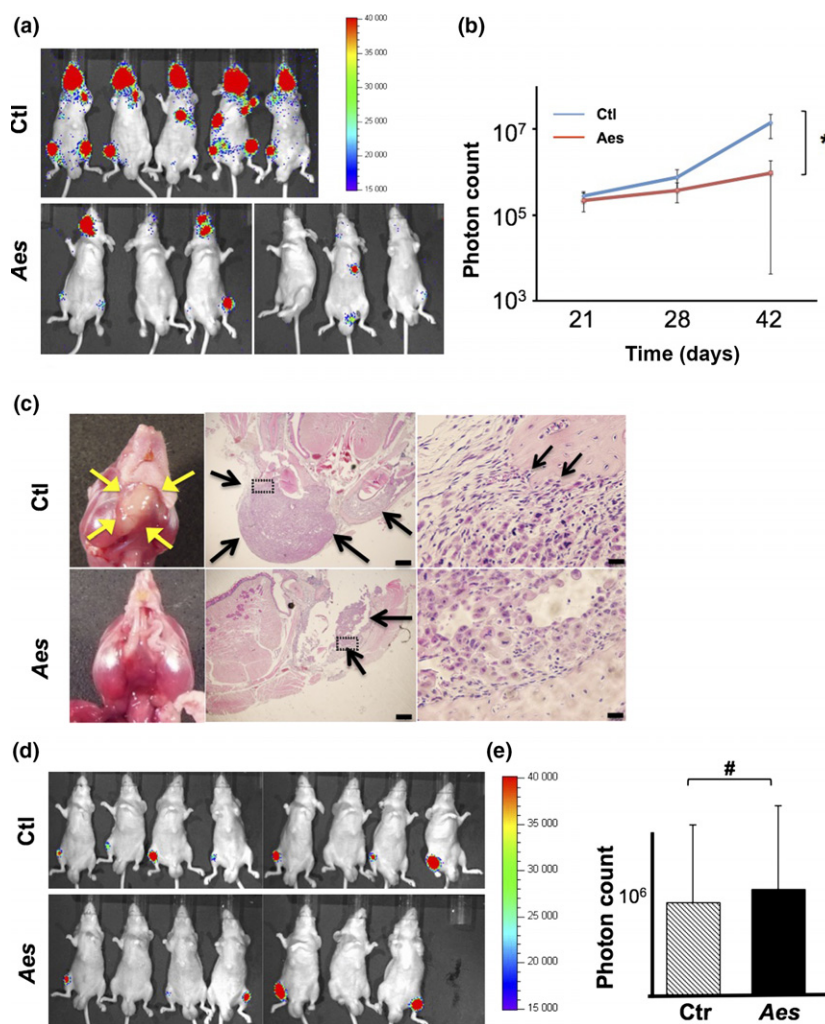


**Fig. 3.** *Aes* suppresses metastatic spread of human PCa cell grafts to the bone in mice. (a) *In vivo* bioluminescence images of mice injected with luciferase-expressing PC3 cells into the left cardiac ventricle. (b) Quantification of the bone metastatic lesions (photon counts) in mice injected with luciferase-expressing PC3 cells as shown in (a). *Aes*, *Aes*-expressing PC3 cells; Ctl, no-*Aes* control cells. (c) Microphotographs of bone metastatic lesions in mice injected with luciferase-expressing PC3 cells into the left ventricle. Arrows indicate metastatic lesions. Framed regions (dotted rectangles) are enlarged on the right. Scale bar; middle 500  $\mu$ m, right 20  $\mu$ m. (d) *In vivo* bioluminescence images of mice injected with luciferase-expressing PC3 cells into femurs directly. (e) Quantification of the bone tumor lesions (photon counts) in mice injected with luciferase-expressing PC3 cells as shown in (d). Asterisk (\*) in (b) indicates statistically significant difference ( $P < 0.05$ ), whereas pound (#) in (e) indicates no statistical significance.

other features of PCa cells than the proliferative properties at the metastatic sites, and that Aes expression is critical for the processes before metastatic colonization.

Taken together, these results with the *in vivo* transplantation and metastasis models suggest that Aes suppresses the ability of PCa cells to progress through the metastatic steps such as invasion, intravasation and extravasation without affecting tumor growth at the primary or metastatic sites.

**Loss of Aes accelerates local microinvasion and lymph node metastasis of Pten-deficient mouse PCa.** Next we investigated whether loss of Aes affects local invasion and distant metastasis of PCa in mutant knock-out mice along the course of progression. At 3 and 6 months of age, we found neither local microinvasion from the primary PIN or cancer to mesenchymal stroma, nor distant metastasis in *Pten* or *Aes/Pten* mice. However, at 12 months, local microinvasion was detectable and it was more frequent in *Aes/Pten* than in *Pten* mice (Fig. 4a,b). Notably, at 18 months of age, we observed lymph node metastasis in 70% (7/10) of *Aes/Pten* mice whereas such metastasis was detected only in 14% (1/7) of *Pten* simple mutant mice of the same age ( $P < 0.05$ , Fig. 4c,d).

As our cell culture analysis showed that AES inhibited Notch signaling, we analyzed Hes1 expression in mouse prostates by IHC. Nuclear Hes1 expression was more prevalent in *Aes/Pten* than in *Pten* mice (Fig. 4e), indicating that *Aes* deletion in *Pten* mice activated Notch signaling.

Snail, EZH2 and MMP9 were reported to be involved in PCa invasion through epithelial-mesenchymal transition (EMT)<sup>(32)</sup>. Expression levels of these proteins were increased in *Aes/Pten* mouse prostates compared with those in *Pten* prostates (Fig. 4f). Additionally, we observed more abundant expression of MMP9 in the prostate of *Aes/Pten* than that of *Pten* mice (Fig. 4g), suggesting more active invasive phenotype of the former mice.

## Discussion

We previously reported that AES suppresses invasion and metastasis of colon cancer through Notch signaling inhibition.<sup>(16)</sup> In this study, we have shown that the same is true with PCa. The present results suggest that loss of AES promotes invasion and metastasis of PCa through Notch activation both in humans and mice. Indeed, we have shown inverse correlation between metastatic spread of PCa and expression of human AES that was markedly suppressed in bone metastasis lesions. Interestingly, Notch pathways were not associated with proliferation of prostate cancer cells as evident by little effect of exogenous AES expression on the proliferation of AR-deficient prostate cancer cells PC3 or DU145.

We have also demonstrated that human AES regulates AR transcriptional activity in PCa cells as reported in the previous studies.<sup>(17,18)</sup> Additionally, our data suggests that AES inhibits

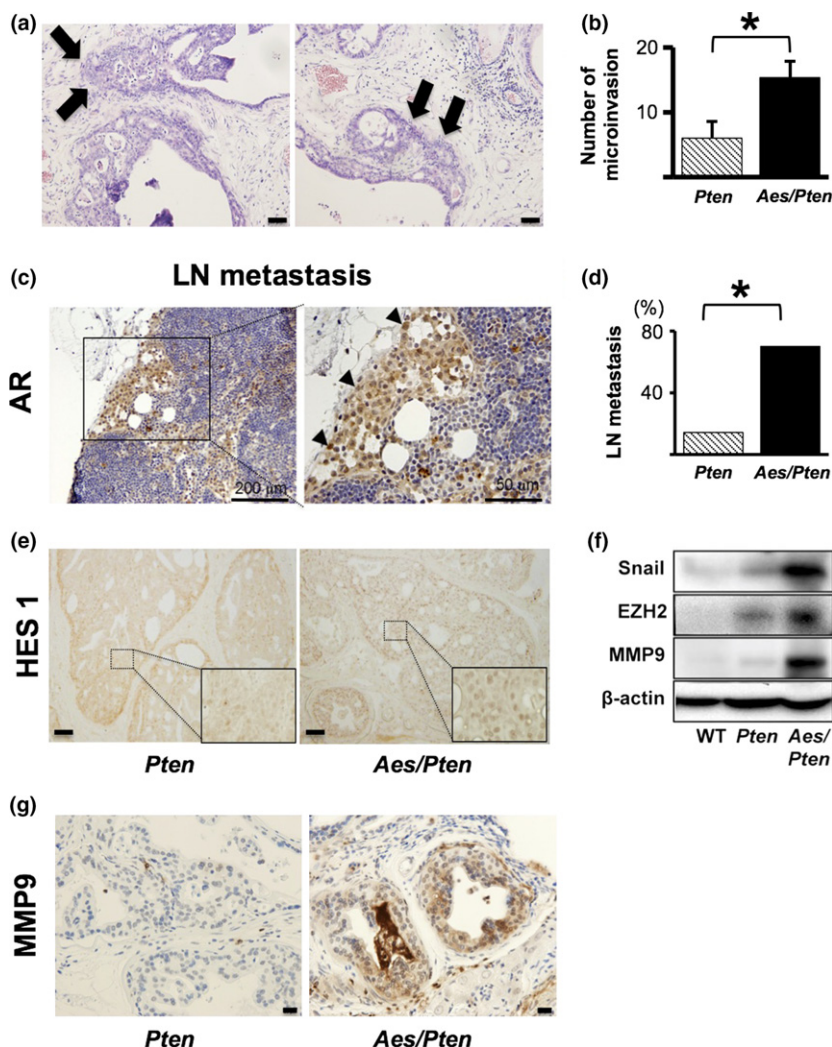


**Fig. 4.** Homozygous *Aes* gene knockout in *Pten*<sup>-/-</sup> mice promotes PCa invasion. (a) Tumor microinvasions (arrows) from PIN lesions into stroma in *Aes/Pten* mice at 12 months of age. (b) Quantification of microinvasion in *Pten* ( $n = 3$ ) and *Aes/Pten* (as shown in A;  $n = 3$ ) mice at 12 months of age. (c) Microphotographs of lymph node metastasis from PCa in *Aes/Pten* mice at 18 months of age detected by immunohistochemistry with anti-AR antibody. (d) Quantification of lymph node metastasis in *Pten* ( $n = 7$ ) and *Aes/Pten* (as shown in C;  $n = 10$ ) mice at 18 months of age. (e) Immunohistochemical staining for Hes1 protein in *Pten* and *Aes/Pten* mouse prostate at 6 months of age. (f) Expression of Snail, EZH2 and MMP9 in the prostates of wild-type (WT) and mutant mice analyzed by western blotting.  $\beta$ -actin was used as the loading control. (g) Immunohistochemical staining for MMP9 in *Pten* and *Aes/Pten* mouse prostates at 6 months of age. Scale bars; (a), 50  $\mu$ m; (c), 200  $\mu$ m (left) and 50  $\mu$ m (right); (e), 20  $\mu$ m; (g), 20  $\mu$ m. Asterisks (\*) in (b) and (d) indicate statistically significant differences ( $P < 0.05$ ).

proliferation and growth of prostate tumors through AR inhibition *in vivo* in a widely used mouse model of PCa caused by prostate-specific *Pten* deletion. Taken together, AES acts as a tumor suppressor targeting both Notch and AR signaling pathways.

These findings have implications in clinical management of castration-resistant PCa (CRPC). Incomplete response to androgen deprivation therapy (ADT) of PCa is attributed largely to insufficient blockade of AR signaling pathway<sup>(3,33)</sup> as demonstrated by the complementary effect of recently developed second-generation androgen-blocking agents.<sup>(34–37)</sup> Stimulating AES may facilitate AR blockade and further strengthen ADT because AES affects AR activity by binding to the N-terminus of AR,<sup>(17,18)</sup> which is distinct from the mode of action by already existing AR-targeting agents. It is conceivable that AES inhibits not only full-length AR but also C-terminus-deficient AR truncate variants. The resistance to the second-generation AR antagonist is often caused by ARV7, one of the commonly expressed variants lacking the ligand-binding and C-terminus domains.<sup>(38)</sup> Further study is needed regarding detailed molecular mechanisms for interaction between ARV7 and AES.

Additionally, our results open the therapeutic possibility of enforcing the AES function to solve current clinical dilemma in PCa treatment. There have been a number of reports showing that ADT induces EMT in PCa cells, and consequently facilitates invasion and metastasis.<sup>(39)</sup> The present results show that AES suppresses EMT and invasion of PCa cells through simultaneous blockade of Notch and AR signaling pathways. Taken together, enforcing the AES function in combination with existing agents for ADT may help overcome drug resistance and treatment-induced metastatic progression of PCa.

Accumulating evidence suggests tumor-promoting functions of Notch signaling pathway in PCa. Several reports suggest that aberrant activation of Notch signaling promotes both invasion and proliferation of PCa through activation of NF- $\kappa$ B or AKT pathway.<sup>(10,11)</sup> Consistently, examinations of clinical samples show that Notch1 and Jagged1 are overexpressed in metastatic lesions of PCa.<sup>(9,12)</sup> However, cytoplasmic molecular mechanisms that activate Notch signaling have not been fully investigated in prostate cancer. The present study has demonstrated that AES functions as an upstream regulator of the Notch signaling also in PCa.

Like in other cancers, EMT is implicated in PCa metastasis. Among a number of EMT markers, only Notch1 is

significantly more abundantly expressed in bone metastases than in primary sites of PCa,<sup>(40)</sup> suggesting that Notch1 might be involved directly in PCa bone metastasis. Another study shows that Snail1 facilitates PCa cell migration and invasion without E-cadherin suppression.<sup>(41)</sup> Furthermore, Snail1 and EZH2 also up-regulate MMPs, which facilitates the invasion of various human cancers including PCa.<sup>(42,43)</sup> Consistently, Snail and MMP9 are more abundantly expressed in *Aes/Pten* than *Pten* mouse prostates, suggesting that decreased AES levels and downstream Notch activation affect EMT of PCa cells (Fig. 4f,g).

Only limited experimental models are available for investigation of PCa bone metastases; for example, intracardiac or intratibial injection of highly transformed tumor cells to induce metastases.<sup>(24,44)</sup> The results of the present study indicate that AES affects the multistep metastatic cascade after intravasation of PCa cells to the blood stream, but before dissemination to the bone.<sup>(45)</sup> The late occurrence of detectable LN metastasis in *Pten* mouse in the present study may be attributable to the strain difference or breeding environment. Indeed, various aggressiveness and progression rates were reported.<sup>(5,20,28,46,47)</sup> In this study, we did not observe metastasis in *Pten* mouse until 18 months of age, which is consistent with a previous report showing that prostate tumors of *Pten*-deficient mouse of C57BL/6 background was slow-growing and showed no metastasis.<sup>(48)</sup> Analyzing more detail role of *Aes* in PCa initiation and progression are expected with multiple other models.

In conclusion, the results of the present study suggest that AES plays roles as tumor and metastasis suppressors in PCa regulating activation of both AR and Notch signaling pathways.

## Acknowledgements

This work was supported by Grant-in-Aid for Scientific Research from the Ministry of Education, Culture, Sports, Science and Technology of Japan (to Y. O. and M. M. T.). The authors thank Teruaki Fujishita, Koji Aoki, Masahiro Aoki, Satoshi Yamashita, Naoki Terada, Noboru Shibasaki, Takeshi Yoshikawa, Takayuki Goto, Yu Miyazaki, Junya Toguchida and Tak W. Mak.

## Disclosure Statement

The authors have no conflicts of interest to declare.

## References

- Siegel R, Ma J, Zou Z, Jemal A. Cancer statistics, 2014. *CA Cancer J Clin* 2014; **64**: 9–29.
- Grönberg H. Prostate cancer epidemiology. *Lancet* 2003; **361**: 859–64.
- Feldman B, Feldman D. The development of androgen-independent prostate cancer. *Nat Rev Cancer* 2001; **1**: 34–45.
- Logothetis C, Lin S-H. Osteoblasts in prostate cancer metastasis to bone. *Nat Rev Cancer* 2005; **5**: 21–8.
- Shen M, Abate-Shen C. Molecular genetics of prostate cancer: new prospects for old challenges. *Gene Dev* 2010; **24**: 1967–2000.
- Chang C, Lee SO, Yeh S, Chang TM. Androgen receptor (AR) differential roles in hormone-related tumors including prostate, bladder, kidney, lung, breast and liver. *Oncogene* 2014; **33**: 3225–34.
- Nantermet PV, Xu J, Yu Y et al. Identification of genetic pathways activated by the androgen receptor during the induction of proliferation in the ventral prostate gland. *J Biol Chem* 2004; **279**: 1310–22.
- Leong KG, Gao WQ. The Notch pathway in prostate development and cancer. *Differentiation* 2008; **76**: 699–716.
- Santagata S, Demichelis F, Riva A et al. JAGGED1 expression is associated with prostate cancer metastasis and recurrence. *Cancer Res* 2004; **64**: 6854–7.
- Bin Hafeez B, Adhami V, Asim M et al. Targeted knockdown of Notch1 inhibits invasion of human prostate cancer cells concomitant with inhibition of matrix metalloproteinase-9 and urokinase plasminogen activator. *Clin Cancer Res* 2009; **15**: 452–9.
- Wang Z, Li Y, Banerjee S et al. Down-regulation of Notch-1 and Jagged-1 inhibits prostate cancer cell growth, migration and invasion, and induces apoptosis via inactivation of Akt, mTOR, and NF-kappaB signaling pathways. *J Cell Biochem* 2010; **109**: 726–36.
- Zhu H, Zhou X, Redfield S, Lewin J, Miele L. Elevated Jagged-1 and Notch-1 expression in high grade and metastatic prostate cancers. *Am J Transl Res* 2013; **5**: 368–78.
- Zayzafoon M, Abdulkadir S, McDonald J. Notch signaling and ERK activation are important for the osteomimetic properties of prostate cancer bone metastatic cell lines. *J Biol Chem* 2004; **279**: 3662–70.
- Brantjes H, Roose J, van De Wetering M, Clevers H. All Tcf HMG box transcription factors interact with Groucho-related co-repressors. *Nucleic Acid Res* 2001; **29**: 1410–9.



- 15 Beagle B, Johnson GV. AES/GRG5: more than just a dominant-negative TLE/GRG family member. *Dev Dyn* 2010; **239**: 2795–805.
- 16 Sonoshita M, Aoki M, Fuwa H *et al.* Suppression of colon cancer metastasis by Aes through inhibition of Notch signaling. *Cancer Cell* 2011; **19**: 125–37.
- 17 Yu X, Li P, Roeder R, Wang Z. Inhibition of androgen receptor-mediated transcription by amino-terminal enhancer of split. *Mol Cell Biol* 2001; **21**: 4614–25.
- 18 Zhang Y, Gao S, Wang Z. Structural and functional analysis of amino-terminal enhancer of split in androgen-receptor-driven transcription. *Biochem J* 2010; **427**: 499–511.
- 19 Taylor B, Schultz N, Hieronymus H *et al.* Integrative genomic profiling of human prostate cancer. *Cancer Cell* 2010; **18**: 11–22.
- 20 Wang S, Gao J, Lei Q *et al.* Prostate-specific deletion of the murine Pten tumor suppressor gene leads to metastatic prostate cancer. *Cancer Cell* 2003; **4**: 209–21.
- 21 Lesche R, Groszer M, Gao J *et al.* Cre/loxP-mediated inactivation of the murine Pten tumor suppressor gene. *Genesis* 2002; **32**: 148–9.
- 22 Jin C, McKeehan K, Wang F. Transgenic mouse with high Cre recombinase activity in all prostate lobes, seminal vesicle, and ductus deferens. *Prostate* 2003; **57**: 160–4.
- 23 Oshima H, Taketo MM, Oshima M. Destruction of pancreatic beta-cells by transgenic induction of prostaglandin E2 in the islets. *J Biol Chem* 2006; **281**: 29330–6.
- 24 Singh A, Figg W. In vivo models of prostate cancer metastasis to bone. *J Urol* 2005; **174**: 820–6.
- 25 Wang Y, Xue H, Cutz J-CC *et al.* An orthotopic metastatic prostate cancer model in SCID mice via grafting of a transplantable human prostate tumor line. *Lab Invest* 2005; **85**: 1392–404.
- 26 Nogawa M, Yuasa T, Kimura S *et al.* Monitoring luciferase-labeled cancer cell growth and metastasis in different in vivo models. *Cancer Lett* 2005; **217**: 243–53.
- 27 Kato H, Taniguchi Y, Kurooka H *et al.* Involvement of RBP-J in biological functions of mouse Notch1 and its derivatives. *Development* 1997; **124**: 4133–41.
- 28 Susan K. Survey of genetically engineered mouse models for prostate cancer: analyzing the molecular basis of prostate cancer development, progression, and metastasis. *J Cell Biochem* 2005; **94**: 279–97.
- 29 Carver BS, Chapinski C, Wongvipat J *et al.* Reciprocal feedback regulation of PI3K and androgen receptor signaling in PTEN-deficient prostate cancer. *Cancer Cell* 2011; **19**: 575–86.
- 30 Sobel RE, Sadar MD. Cell lines used in prostate cancer research: a compendium of old and new lines—part 1. *J Urol* 2005; **173**: 342–59.
- 31 Kim SH, Sehwat A, Sakao K, Hahm ER, Singh SV. Notch activation by phenethyl isothiocyanate attenuates its inhibitory effect on prostate cancer cell migration. *PLoS ONE* 2011; **6**: e26615.
- 32 Nelson PS. Targeting the androgen receptor in prostate cancer—a resilient foe. *N Engl J Med* 2014; **371**: 1067–9.
- 33 Kobayashi T, Inoue T, Kamba T, Ogawa O. Experimental evidence of persistent androgen-receptor-dependency in castration-resistant prostate cancer. *Int J Mol Sci* 2013; **14**: 15615–35.
- 34 Scher HI, Fizazi K, Saad F *et al.* Increased survival with enzalutamide in prostate cancer after chemotherapy. *N Engl J Med* 2012; **367**: 1187–97.
- 35 Beer TM, Armstrong AJ, Rathkopf DE *et al.* Enzalutamide in metastatic prostate cancer before chemotherapy. *N Engl J Med* 2014; **371**: 424–33.
- 36 de Bono JS, Logothetis CJ, Molina A *et al.* Abiraterone and increased survival in metastatic prostate cancer. *N Engl J Med* 2011; **364**: 1995–2005.
- 37 Ryan CJ, Smith MR, de Bono JS *et al.* Abiraterone in metastatic prostate cancer without previous chemotherapy. *N Engl J Med* 2013; **368**: 138–48.
- 38 Antonarakis ES, Lu C, Wang H *et al.* AR-V7 and resistance to enzalutamide and abiraterone in prostate cancer. *N Engl J Med* 2014; **371**: 1028–38.
- 39 Clyne M. Prostate cancer: androgen deprivation causes EMT in the prostate. *Nat Rev Urol* 2012; **9**: 4.
- 40 Seema S, Jill M, Wei C, Fazlul HS. Molecular signature of epithelial-mesenchymal transition (EMT) in human prostate cancer bone metastasis. *Am J Transl Res* 2010; **3**: 90–9.
- 41 Barrallo-Gimeno A, Nieto MA. The Snail genes as inducers of cell movement and survival: implications in development and cancer. *Development* 2005; **132**: 3151–61.
- 42 Olmeda D, Jordá M, Peinado H, Fabra A, Cano A. Snail silencing effectively suppresses tumour growth and invasiveness. *Oncogene* 2007; **26**: 1862–74.
- 43 Shin YJ, Kim J-HH. The role of EZH2 in the regulation of the activity of matrix metalloproteinases in prostate cancer cells. *PLoS ONE* 2012; **7**: e30393.
- 44 Corey E, Quinn J, Bladou F *et al.* Establishment and characterization of osseous prostate cancer models: intra-tibial injection of human prostate cancer cells. *Prostate* 2002; **52**: 20–33.
- 45 Valastyan S, Weinberg RA. Tumor metastasis: molecular insights and evolving paradigms. *Cell* 2011; **147**: 275–92.
- 46 Aytes A, Mitrofanova A, Kinkade CW *et al.* ETV4 promotes metastasis in response to activation of PI3-kinase and Ras signaling in a mouse model of advanced prostate cancer. *Proc Natl Acad Sci U S A* 2013; **110**: E3506–15.
- 47 Wang J, Kobayashi T, Floc'h N *et al.* B-Raf activation cooperates with PTEN loss to drive c-Myc expression in advanced prostate cancer. *Cancer Res* 2012; **72**: 4765–76.
- 48 Svensson RU, Haverkamp JM, Thedens DR, Cohen MB, Ratliff TL, Henry MD. Slow disease progression in a C57BL/6 pten-deficient mouse model of prostate cancer. *Am J Pathol* 2011; **179**: 502–12.

## Supporting Information

Additional Supporting Information may be found online in the supporting information tab for this article:

**Fig. S1.** Immunohistochemical evaluation of AES expression in human PCa specimens.

**Fig. S2.** AES expression in normal prostate, and primary and metastatic PCa tissues.

**Fig. S3.** Immunohistochemistry of AES in bone metastatic lesions of human PCa.